# On the Multiresolution Randomization of Coherent Inflaton Energy & Entropy Flow

Jonathan Braden and J. Richard Bond
Department of Physics, University of Toronto / Canadian Institute for Theoretical Astrophysics

## Abstract

*After inflation the coherent energy of the inflaton field must ultimately be transferred into the incoherent energy density of Standard Model particles to begin the hot big bang. In many models, the early stages of this energy transfer are very efficient due to instabilities that arise when the inflaton couples to other fields. This rapid transfer of energy, known as preheating, leads to energy distributions that are sharply peaked in the infrared. In order to connect the end of inflation to the standard hot big bang, we need to understand the evolution from this highly nonequilibrium state to thermal equilibrium.*

*We study thermalization in a preheating model driven by parametric resonance with large parallel simulations using a modified version of the lattice code DEFROST [1]. Shortly after nonlinear effects terminate the resonance, the fields enter into a slowly evolving phase during which nearly stationary one-point distributions of the energy density emerge and the density power spectrum develops a slowly moving peak whose height increases linearly with time as the overall fluctuations in the system grow. We introduce a nonequilibrium entropy with contributions from all wavenumbers to measure the growing complexity in the system. We also use a hierarchical coarse-graining via block-smoothing (akin to Wilson's Renormalization Group analyses of lattice calculations) to study the scale dependence of the energy density and show there is a rapid buildup in an intermediate range of scales. Our results indicate that within the multifield complexity prior to thermalization there are underlying entropic principles guiding the inexorable cascade to short distances, the universality of which remains to be explored.*

## Model

We consider a simple model for preheating after chaotic inflation with lagrangian

$$\mathcal{L} = -\frac{1}{2}\partial_\mu\phi\partial^\mu\phi - \frac{1}{2}\partial_\mu\chi\partial^\mu\chi - \frac{1}{2}m^2\phi^2 - \frac{g^2}{2}\phi^2\chi^2 .$$

After inflation, the inflaton $\phi$ oscillates around the minimum of its potential leading to parametric amplification of $\chi$ fluctuations. Eventually backreaction of these fluctuations ends the resonance and leads to a breakup of inflaton coherence and the onset of the slowly evolving nonlinear stage [2,3].

## Hints of Simple Dynamics

During the nonlinear stages, the one-point distributions of the stress-energy tensor components become nearly stationary. In particular, we find the normalized energy density approaches a log-normal distribution and the normalized components of the energy current become nearly Gaussian. This evolution to such a broad brush-stroke low order result suggests we should look for a simple principle underlying the dynamics.

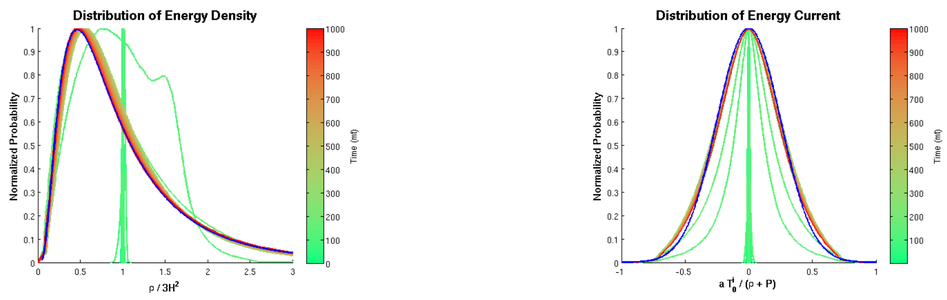


Fig. 1: Left: Distribution of energy densities $\frac{\rho}{3H^2}$ for a range of times, where $3H^2 = \bar{\rho}/M_P^2$ is the box averaged squared Hubble parameter. The blue line is a log-normal fit at $mt = 1024$. Right: Distribution of energy current, again showing a very slow evolution at late time. The blue line is a Gaussian fit at $mt = 1024$. In both figures, the probabilities have been normalized to their maximum value (we plot $P(t)/P_{max}(t)$).

## The Energy Cascade

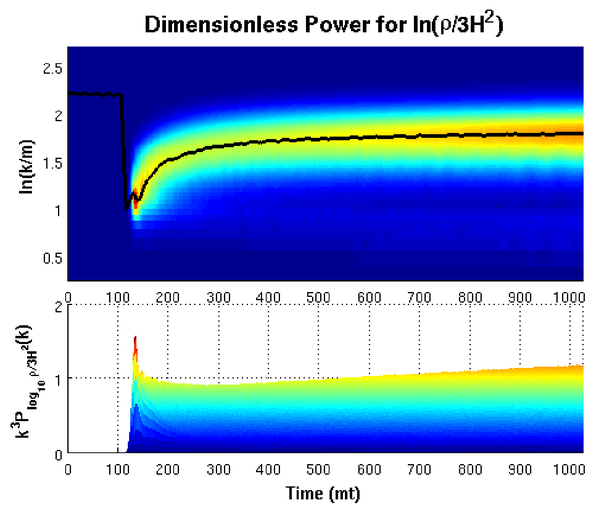


Fig. 2: Evolution of the dimensionless power spectrum of $\log(\rho/3H^3)$ with the location of the peak indicated by the black line.

The parametric resonance mentioned above leads to exponential growth of modes with $k \sim ma$. This results in a sharp peak in the power spectrum that becomes visible at $mt \sim 100$. Shortly after this peak becomes nonlinear, it rapidly shifts to shorter wavelengths. This is followed by a much longer stage of nonlinear evolution where the peak slowly moves to larger comoving wavenumbers. A remarkable feature of this stage is the linear growth of the peak height with time.

## Entropy Production

The nonequilibrium entropy of a random field $f(x)$ with probability density functional $\mathcal{P}[f(x)]$ is a functional integral over all configurations,

$$S = -\int \mathcal{D}f\mathcal{P}[f]\ln\mathcal{P}[f] .$$

For a field subject to the constraint that only its covariance matrix C, with eigenvalues P(**k**), has been measured, the resulting entropy is

$$\begin{aligned}\frac{S}{N^3} &= \frac{1}{2} + \frac{1}{2}\ln(2\pi) + \frac{1}{2N^3}\ln(\det C) \\ &= \frac{1}{2} + \frac{1}{2}\ln(2\pi) + \frac{1}{2N^3}\sum_{\mathbf{k}}\ln(P(\mathbf{k})) .\end{aligned}$$

This is also what one gets if $\mathcal{P}[f(x)]$ is Gaussian, but we are not assuming that all higher point correlations vanish, just that they are not observed to constrain the degrees of freedom of the ensemble. Here we will take $\ln(\rho/3H^2)$ to be our dynamical field, where $3H^2 = \bar{\rho}/M_P^2$ is the box averaged squared Hubble parameter. Thus, $\rho$ is normalized to its mean value. Taking only the covariance matrix to be measured, we find the entropy behaves as shown to the right. There is a rapid production of entropy at $mt \sim 100$ when the fields first go nonlinear. This is followed by a much longer stage in which the entropy increases much more slowly as the field attempts to equilibrate.

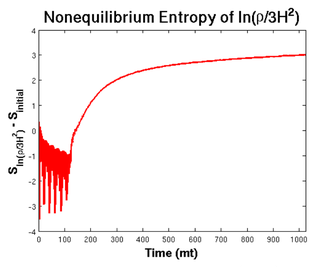


Fig. 3: The entropy of $\ln\left(\frac{\rho}{3H^2}\right)$ assuming that only the covariance matrix has been measured. Here we have normalized the result by subtracting the entropy of the initial field configuration on the lattice. The initial decrease is due to the adiabatic evolution of the high frequency modes, which we have not accounted for by only subtracting off the initial entropy.

## Buildup of Fluctuations with Scale

We now study the scale dependence of our system in real space using a simple renormalization procedure. Given a cubic lattice with $N^3$ points and grid spacing $dx$, we define a new lattice of size $\left(\frac{N}{2}\right)^3$ and spacing $2dx$ by grouping $2x2x2$ cubes of sites together to form a single new site. We define smoothed fields on the new lattice by averaging over the 8 lattice sites making up each cube.

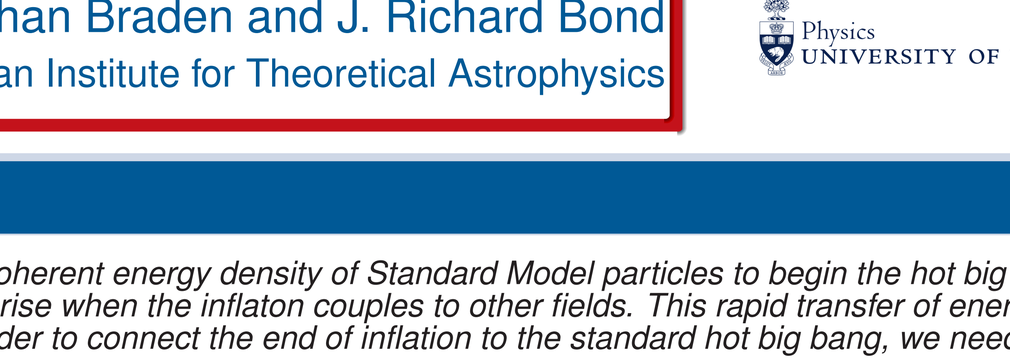


Fig. 4: Left: Distribution of energy density as we vary the lattice spacing $mdx$. Right: Time evolution of the variance of $ln(\rho_{mdx}/3H^2)$ for various smoothing scales. Here, $\rho_{mdx}$ is the smoothed density field on a lattice with grid spacing $mdx$.

The figures above illustrate the buildup of density fluctuations smoothed by this procedure as resolution increases. Initially, the width of the distribution grows at an increasing rate and as a result shifts to the left. However, as we continue to resolve finer structure past $mt \sim 20/512$, the distribution changes much more slowly. In the right hand panel above, we see that the variances in $\ln(\rho/3H^2)$ obey a simple linear evolution at late times. Since our smoothed energy densities provide us with a definition of the local background energy density, we can study fluctuations around these local backgrounds, as in the figure below. At the time of the onset of nonlinearity, the fluctuations at scales $mdx \sim 40/512$ change much more dramatically than those at smaller scales. However, after this rapid evolution, the distributions at these larger scales quickly settle down and become nearly stationary. The smaller scale distributions, on the other hand, continue to grow. A plausible explanation (to be further explored) is that the energy flows from large to small packets as the system is drawn towards equilibration - although we are very far from that state in these simulations. The flux has only reached a steady state at the larger scales.

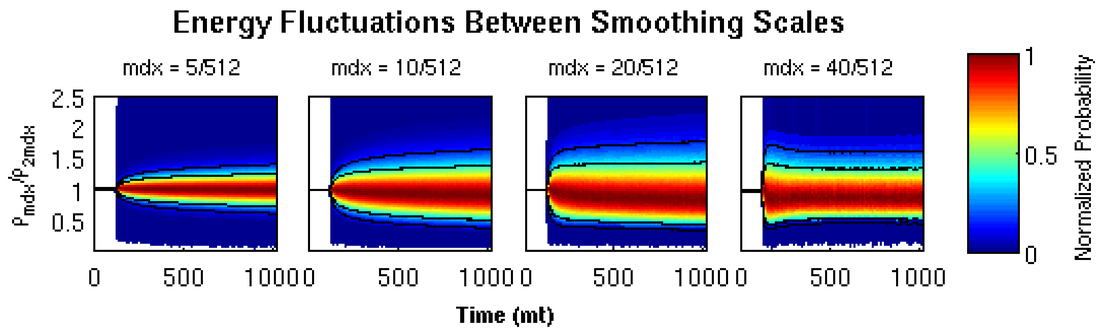


Fig. 5: The distribution of fluctuations in energy densities between successive coarse-graining scales. The probability distributions have been normalized to their maximum values. The locations where the distribution drops to $e^{-1}$ and $e^{-2}$ of its maximum value are indicated by the black lines. The coloured regions indicate the extremal values.

## Evolution at a Single Lattice Site

The previous sections focussed on properties of the density distribution over the lattice at a fixed moment of time. The time dependence of the field fluctuations can shed light on how energy is being transported. As the system evolves, the collective phonon modes of the total energy density become of greater significance than the highly entangled $\phi$ and $\chi$ fields, but the dispersion relation is that of a light field, with a near speed-of-light sound speed, in spite of the large nonlinear corrections to the effective mass. This suggests that the energy may flow rapidly, decohering the time-time correlations at a fixed lattice site. To illustrate this behaviour, the figures below show that the density at a fixed lattice site indeed fluctuates at all times rather than settling down into a steady state, indicating that energy is still being transported between lattice sites. The right hand figure shows the fluctuations in density are larger on scales $mdx \sim 40$ than on smaller scales, in agreement with the findings in the previous section.

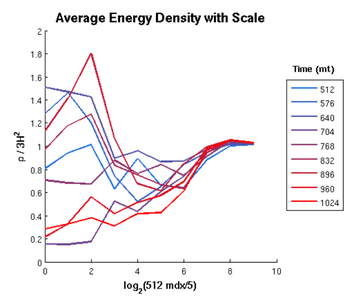


Fig. 6: Energy density at a fixed lattice site as a function of smoothed lattice size.

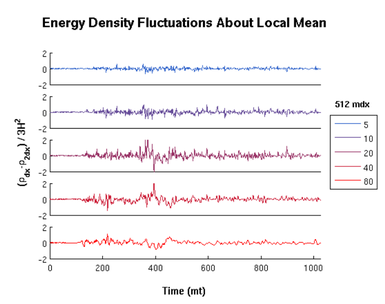


Fig. 7: Density fluctuations around the local mean for several different smoothing scales.

## References and Acknowledgements

[1] Frolov, A., JCAP 0811:009 (2008), arXiv:0809.4904 [hep-ph]
[2] Kofman, L *et al*, Phys. Rev. D56: 3258-3295 (1997), hep-ph/9704452
[3] Podolsky, D. *et al*, Phys. Rev. D73: 023501 (2006), hep-ph/0507096
[4] Misha, R. and Tkachev, I., Phys. Rev. D70: 043538 (2004), hep-ph/0403101

This work was supported by NSERC, OGS and the University of Toronto.